SHEAR WAVE PROPAGATION INDUCED BY A LOCALIZED RADIATION FORCE: COMPARISON BETWEEN THEORY AND INTERFEROMETRIC LASER MEASUREMENTS

S. Callé, J.P. Remenieras, O. Bou Matar and F. Patat
LUSSI / GIP Ultrasons FRE CNRS 2448, Faculté de médecine, Tours, FRANCE
calle_s@med.univ-tours.fr

Abstract

Radiation force is usually used as stress source in dynamic elastography imaging methods. However, displacements induced by this stress field are generally not precisely known in terms of spatial repartition and temporal evolution.

A model based on the elastodynamic Green function describing the shear waves generated by focused ultrasound is developed. The shear wave displacements are described by the spatial and temporal convolution of this Green function with the localized stress field. For propagation distances in the order of the shear wavelength, the predominant term in the Green function expression is the near-field term. The total displacement is the summation of all the Green functions expressed at each point of the stress source. We studied the evolution of the shape of the displacement/time curves as a function of the shear elastic modulus. When this coefficient increases, the maximum amplitude of displacement and the time to achieve this maximum decrease, but the slope of the displacement/time curve increases.

An optical interferometric method allowed us to measure experimentally these shear displacements. A tissue-mimicking phantom including a thick metallized sheet is placed in water. When the transducer focalizes on the reflective sheet, we measure with the laser probe displacements due to the radiation force.

The previously described theoretical profiles agree with the experimental curves.

Introduction

In soft biological tissue, the shear elasticity modulus μ is ten order of magnitude smaller than the compression elasticity modulus $\mathrm{K} = \lambda + 2/3\mu$. In this particularly medium, the Young modulus $\mathrm{E} = 9\mathrm{K}\mu/(3\mathrm{K} + \mu)$ is approximately 3μ, and is then linearly proportional to the shear elasticity modulus. This Young modulus is manually estimated by clinician during breast palpation medical exam. The success of breast palpation is due to the fact that the shear elasticity modulus of the breast lesion is an order of magnitude greater than normal breast tissue [1]. However, limits of this manual exam lie in the fact that the sensibility of the breast lesion detection decreases with depth and that the detection is only possible for lesions with important size. Recently, new imaging methods named acoustic remote palpation [2] or shear wave elasticity imaging [3], enable to image local variations of the mechanical properties of tissue, have been proposed. In these methods, high intensity focused ultrasounds are used to apply a highly-localized radiation force within tissue. These techniques probe the elasticity of the internal regions of the tissue with a "virtual finger". The purpose of this paper is to calculate the tissue displacement $\vec{u}(\vec{x},t)$ induced by the elastic waves propagation generated by this impulse stress field. Our theoretical results will be compared to those obtained experimentally in a tissue-mimicking phantom with an optical method.

Theory

We are seeking to solve the displacement $\vec{u}$ that is solution to the elastic-wave equation with an unidirectional force $\vec{f}$ in a homogeneous, isotropic, unbounded solid medium. The elastodynamic equation to be solved for $\vec{u}$ is given by the expression:

$$\rho\ddot{\vec{u}} = \vec{f} + (\lambda + 2\mu)\vec{\nabla}\left(\vec{\nabla}.\vec{u}\right) - \mu\vec{\nabla}\times\left(\vec{\nabla}\times\vec{u}\right) \qquad (1)$$

where $\vec{f}(\vec{x},t)$ denotes the force acting per unit volume on the particle originally at position $\vec{x}$ at some reference time. In our biological application, the source $\vec{f}$ extends over a finite volume V and is applied throughout the focal region of the acoustic beam. If scattering, diffraction, and non-linearity [4] effects are neglected, and suppose that the radiation force originates in attenuation, $f_i(\vec{x},t)$ is applied only in the ultrasound beam direction x_j and can be expressed as follow [5]:

$$f_i(\vec{x},t) = X_0(t)F(\vec{x})\delta_{ij} \text{ with } F(\vec{x}) = 2\alpha I(\vec{x})/c_L \qquad (2)$$

where $\alpha\left[\mathrm{m}^{-1}\right]$ is the absorption coefficient in the tissue, and $\mathrm{I}\left[\mathrm{W}/\mathrm{cm}^2\right]$ is the temporal average intensity of the acoustic ultrasound beam. Since the beam is focused, the amplitude of the force strongly varies around the focus zone. We denote by $X_0(t)$ the temporal evolution of the source and δ_{ij} the Kronecker delta function signifying the directional property that $f_i = 0$ for $i \neq j$. The i^{th} component of the displacement (eq. 3) is given by the convolution of the Green function g_{ij} with the force source [6].

$$u_i(\vec{x},t) = g_{ij}(\vec{x},t) \underset{\text{3D Space}}{\otimes} f_j(\vec{x}) \underset{\text{Time}}{\otimes} X_0(t) \tag{3}$$

with:

$$g_{ij}(\vec{x},t) = \frac{1}{4\pi\rho_0}\left(3\gamma_i\gamma_j - \delta_{ij}\right)\frac{1}{r^3}\int_{r/c_l}^{r/c_t} \tau\delta_0(t-\tau)\,d\tau + \frac{1}{4\pi\rho_0 c_l^2}\gamma_i\gamma_j\frac{1}{r}\delta_0\left(t-\frac{r}{c_l}\right) - \frac{1}{4\pi\rho_0 c_t^2}\left(\gamma_i\gamma_j - \delta_{ij}\right)\frac{1}{r}\delta_0\left(t-\frac{r}{c_t}\right) \tag{4}$$

In this Green function, the relative magnitude of the different terms depends on the source-receiver distance $r = |\vec{x} - \vec{\varsigma}|$. $\gamma_i = (x_i - \varsigma_i)/r$ are direction cosines referred to the source position $\vec{\varsigma}$. c_t and c_l are the shear and compression wave celerity defined by $c_l^2 = (\lambda + 2\mu)/\rho$ and $c_t^2 = \mu/\rho$. The first term behaves like r^{-2} for times that are shorts compared to $r/c_t - r/c_l$, and the remaining terms behave like r^{-1}. Since r^{-2} dominates r^{-1} as $r \to 0$, the term $r^{-3}\int_{r/c_l}^{r/c_t} \tau\delta_0(t-\tau)\,d\tau$ is called the "*near-field*" term, and the two others term are called the "*far-field*" terms. For an impulse spatial source distribution located at $\vec{\varsigma} = \vec{0}$, the displacement duration corresponds to the time of flight of the shear wave which propagates from the position of the force to the position of the receiver situated at $\vec{x}$. Inside the source, the predominant term is the "near-field" term, and we can determine analytically the maximum of the displacement $M = F_0/4\pi\rho_0 r^2 c_t$ calculated for the time $t = r/c_t$. This amplitude depends on the force amplitude F_0, and is inversely proportional to the shear elasticity modulus. We can determine $\Sigma = F_0/4\pi\rho_0 r$, the slope of the curve which is linearly proportional to the force amplitude F_0, and independent of the shear celerity.

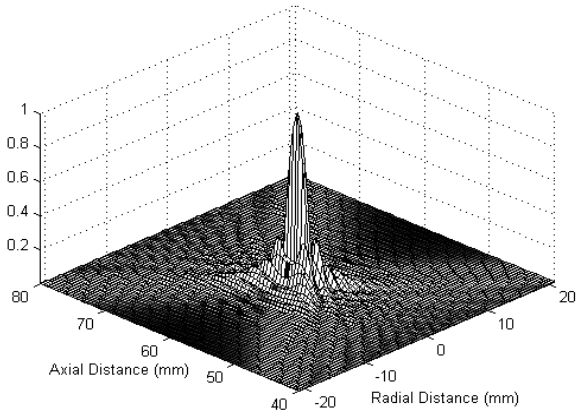

Figure 1: Focused ultrasound radiation force distribution induced by a focused transducer operating at 1MHz with $a = 4.16$ cm and $d = 6$ cm.

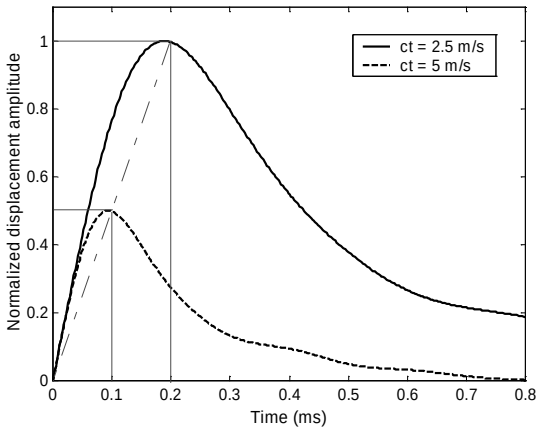

Figure 2: Impulse tissue displacement for two different c_t.

At high frequencies, the tissue can be considered as a liquid medium. We used a classical angular spectral decomposition associated with a source condition described by Levin *et al.* [7] for the calculation of the ultrasound pressure generated by the focalized transducer. Figure 1 shows the normalized amplitude of the radiation pressure, computed using the square of the envelope of the ultrasound pressure for $\vec{x}$ varying in the $(x_1, x_2 = 0, x_3)$ plan. With the specifications of the transducer used in the experimental part of this paper, the radiation force is well localized in space, and measures 6mm in the axial direction, and 2mm in the radial direction. Figure 2 shows the impulse displacement $u_3(\vec{x},t)$ at the position $\vec{x} = \left(0.5\times10^{-3}, 0, 0\right)$, with a temporal impulse excitation $X_0 = \delta(t)$. This displacement was computed for two different shear celerities, $c_t = 5$ m/s and $c_t = 2.5$ m/s. Each curve is simply the spatial convolution of all the elementary source points, and then the sum of the triangular contributions of each point. The displacement duration is the propagation time of the shear wave from the farther source point to the receiver. The maximum amplitude of the displacement curve M is a complex combination of the source geometry, the shear wave celerity c_t, and the amplitude F_0 of the radiation force. For a given source spatial profile, if the geometry and the amplitude of the radiation force remain constant, the parameter M can give information on the shear elasticity modulus. The time τ corresponding to the duration of the rising edge is an important parameter since it is proportional for a fixed source configuration to the shear wave propagation time and then to the shear elasticity modulus μ. As we predict from the elementary source point, the slope of the curve Σ is the same for the two different shear celerities, and we only have a stretch of the coordinates in the two dimensions, due to the difference between the shear celerities. Figure 3 shows the displacement $u_3(\vec{x},t)$ at

the same spatial position, for a shear celerity $c_t = 5\,\text{m/s}$, for different excitation durations $X_0(t)$. The effect of saturation of the displacement is clearly shown for the excitation duration $T = 5\,\text{ms}$. Figure 4 illustrates the tissue displacement with a $200\,\mu\text{s}$ excitation duration for two different shear celerities. The temporal convolution deforms the curves and the proportionality of figure 2 is lost. The slope Σ of the curves are not the same, and the rising edge time τ is no more proportional to the difference between the shear celerities. We then can envisage a deconvolution procedure on our experimental data to compensate the effects of the finite duration of the emission.

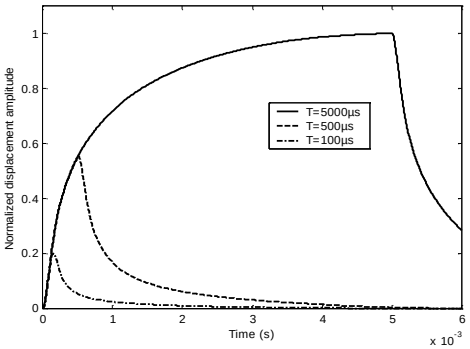

Figure 3: Tissue displacement for different times of emission $X_0(t)$ with $c_t = 5\,\text{m/s}$.

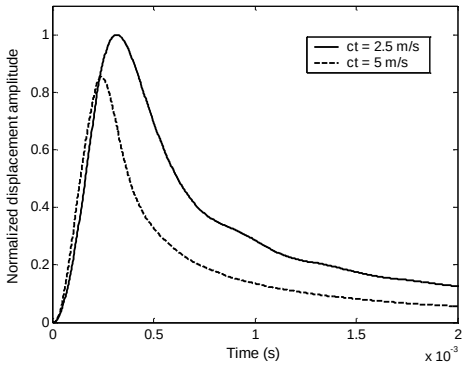

Figure 4: Tissue displacement for different shear celerities with a emission duration of $200\,\mu\text{s}$.

Experimental results

Figure 5 represents the experimental set-up. A tissue-mimicking (3) phantom (gel with 8% gelatine) including a $1\mu\text{m}$-thick metallized sheet of Mylar (2) is placed in a water tank (6). While the transient shear wave propagates, this reflective target moves with the tissue. The central plane of the phantom was positioned between the transducer (1) and the optical interferometer (5), perpendicular to both ultrasonic and laser beams. The $8.32\,\text{cm}$ diameter transducer emitting at 1MHz focalizes at $6\,\text{cm}$ at the optical focal point. The laser probe is a compact Mach-Zender heterodyne interferometer. The laser beam enters the water tank through an optical window (4) specially coated for the YAG wavelength to avoid reflections, propagates in the tissue-mimicking phantom, and is reflected back by the sheet of Mylar. The displacement of the Mylar sheet, induces by the ultrasound radiation force, makes a phase modulation of the laser beam. The optical phase-shift $\Delta\Phi$ is given by $\Delta\Phi = (4\pi/\lambda)u(t)$, where $u(t)$ is the displacement at the sheet surface. This technique allows us to measure the high frequency displacements associated with the ultrasound wave, and the low frequency deformations created by the radiation force. A high frequency filtering allows us to suppress the high frequency component of the signal.

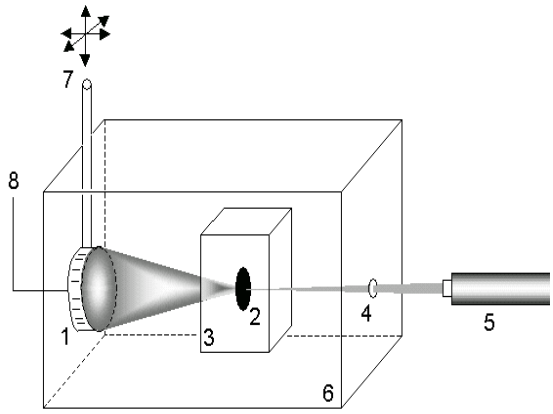

Figure 5: Experimental set-up.

Figure 6 presents an example of the displacement induced by the radiation force before filtering. The US emission begins at $0.5\,\text{ms}$ (1). After $40\,\mu\text{s}$, which corresponds to the time propagation between the transducer and the sheet of Mylar, we can see the US wave (in the present case, 300 periods at 1MHz), which rapidly moves the reflective target. From this HF displacement (2) the acoustical HF pressure at the focal point of the transducer (in the present study $4.2\,\text{MPa}$) can be calculated. The constant radiation force created by a constant averaged pressure at the focal point induce the tissue displacement (3). This displacement is followed by a period of relaxation (4).

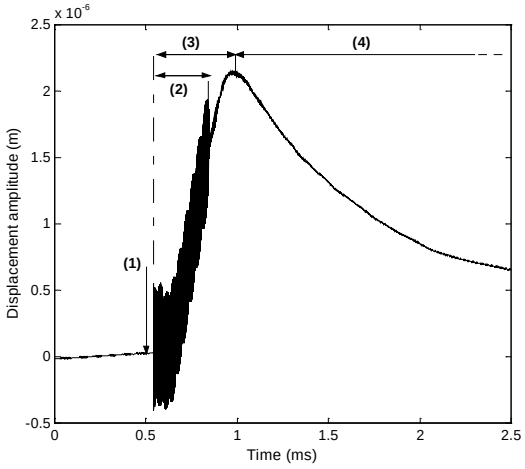

Figure 6: Experimental measurement of the displacement induced by the radiation force.

The displacement induced by the radiation force is $2\mu m$ with a $2nm$ signal to noise ratio, whereas ultrasonic methods based on inter-correlation techniques classically have a $0.8\mu m$ noise level. Figure 7 represents the radiation force for an emission burst duration varying from 100 to 600 periods at 1MHz (*i.e.* between $0.1ms$ and $0.6ms$). As predicted by theory, the displacement amplitude depends on the high frequency burst duration $X_0(t)$. The saturation effect is not apparent because the displacement amplitude remains small. Figure 8 presents the displacement for different emission tension amplitudes U (varying from $20V$ to $50V$ pic to pic). When U increases, the displacement amplitude of the tissue increases. The rising time τ of the displacement curve remains constant as shown theoretically.

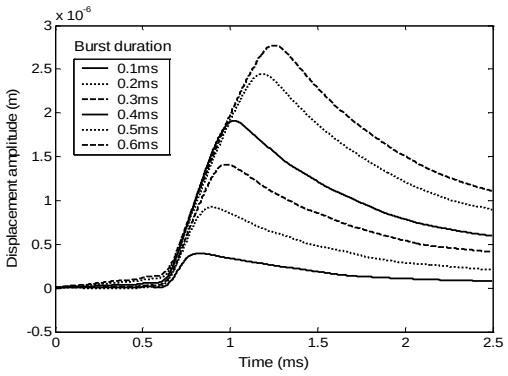

Figure 7: Tissue displacement as a function of the high frequency burst duration $X_0(t)$.

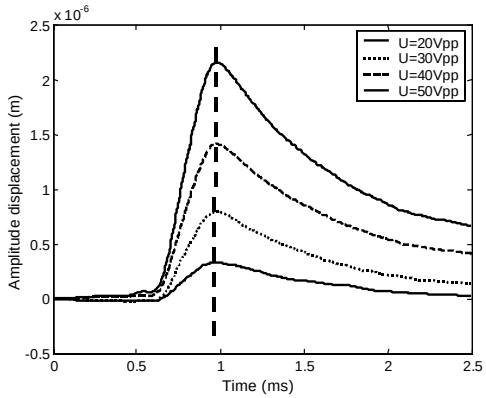

Figure 8: Tissue displacement as a function of the amplitude of the radiation force F_0.

Figure 9 compares the theory previously exposed with an experimental measurement. The emission begins at $500\mu s$. In the theoretical curve, the shear velocity is fixed at $c_t = 1.3m/s$. In both cases, the emission duration is $500\mu s$. The theoretical profile agrees with the experimental curve.

Conclusion

In this paper, the importance of the source geometry and the *"near-field"* term of the elastodynamic Green function on the calculation of the temporal deformation induced by ultrasound radiation pressure are highlighted. The expression of the displacement $\vec{u}(\vec{x},t)$ is simply the convolution of this Green function by the spatial force source and the temporal evolution of the ultrasound emission. The shape of the displacement has been studied for different shear wave celerities, different emission times and different amplitudes of the radiation force. The importance of parameters obtained directly from the displacement curves as the maximum amplitude M, the time τ corresponding to the duration of the rising edge and the slope Σ of the displacement curves has been studied experimentally and theoretically. With an adapted temporal deconvolution technique, used to compensate the deformation effect linked to the finite duration of the emission $X_0(t)$, the rising time τ of the displacement curves seems to be a robust parameter to form an image directly proportional to the shear elasticity modulus μ.

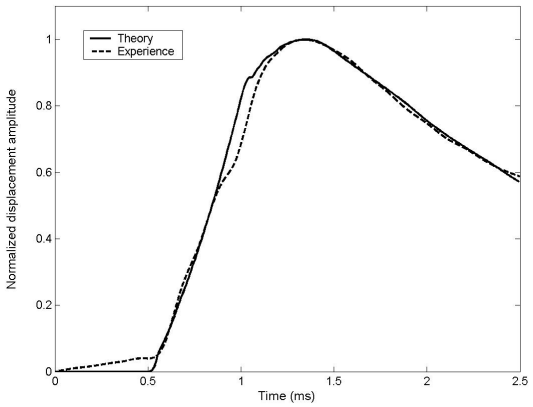

Figure 9: Comparison between theory and experience.

References

[1] A.P. Sarvazyan *et al.*, "Biophysical bases of elasticity imaging", Acoustical Imaging, vol. 21, pp. 223-240, 1995.

[2] K. Nigntingale *et al.*, "On the feasibility of remote palpation using acoustic radiation force", J. Acoust. Soc. Am., vol.110, pp.625-634, 2001.

[3] A.P. Sarvazyan *et al.*, "Shear wave elasticity imaging: a new ultrasonic technology of medical diagnostics", Ultrasound in Med. & Biol., vol. 24, pp. 1419-1435, 1998.

[4] O.V. Rudenko, A.P. Sarvazyan, S.Y. Emilianov, "Acoustic radiation force and streaming induced by focused nonlinear ultrasound in a dissipative medium", J. Acoust. Soc. Am., vol.99, pp.2791-2798, 1996.

[5] P.J. Westervelt, "The theory of steady force caused by sound waves", J. Acoust. Soc. Am., vol. 23, pp. 312-315, 1951.

[6] K. Aki and P.G. Richards, Quantitative seismology – Theory and methods, W.H. Freeman and Company, 1980.

[7] V.M. Lobkis, O.I. Maev and R.G. Maev, "Field of a spherical focusing transducer with arbitrary aperture angle", Sov. Phys. Acoust., vol. 33, 1987.